Complex Formation in an Aqueous $ZnBr_2$ Solution Based on Electron Diffraction, X-ray Scattering and Raman Spectra

E. Kálmán, I. Serke, G. Pálinkás
Central Research Institute for Chemistry, Budapest
G. Johansson
Royal Institute of Technology, Stockholm
G. Kabisch
Arbeitsstelle der Sächsischen Akademie, Freiberg
M. Maeda, H. Ohtaki
Tokyo Institute of Technology, Japan

Z. Naturforsch. **38 a,** 225–230 (1983); received September 30, 1982

Dedicated to Professor Alfred Klemm on the occasion of his 70th birthday

Electron and X-ray scattering as well as Raman spectra of as aqueous solution of $ZnBr_2$ with a Br^-/Zn^{++} ratio of 3 : 1 have been studied. The existence of hexaaquo, di-, tri- and tetra-bromo complexes in solution has been established by all three methods. Octahedral hexaaquo and tetrahedral $Zn(H_2O)_{4-n}Br_n$ complexes with $n = 2, 3, 4$ are consistent with electron and X-ray structure functions. The inner sphere type complexes have interatomic distances of 2.2 Å for Zn^{++}–H_2O, 2.4 Å for Zn^{++}–Br^-, 3.93 Å for Br^-–Br^- and 2.91 Å for W–W interactions with average numbers of contacts 2.4, 2.22, 1.33 and 1.1 respectively.

1. Introduction

An earlier X-ray study [1] of nine concentrated aqueous $ZnBr_2$ solutions indicated, based on the analysis of the areas under the peaks in the radial distribution functions, that the Zn^{++} ion is coordinated by two bromide and two water molecules. It also showed that the zinc ion becomes totally four coordinated by bromide if the bromide/zinc ratio increases by the addition of hydrobromic acid. The concentration in Zn^{++} of the solutions investigated ranged from 3.5 up to 17.7 molal for $Br^-/Zn^{++} = 2$ and from 4.2 up to 23 molal at higher Br^-/Zn^{++} ratios. Interatomic distances for Zn^{++}–Br^-, Br^-–Br^- and Br–W contacts were found to be at 2.4 Å, 3.9 Å and 3.2 Å respectively. The tetrahedral symmetry of the complexes was suggested.

A study [2] of the variation in the Raman spectra of zinc bromide solutions with the Br^-/Zn^{++} ratio, maintaining the total concentration of Zn^{++} and Br^- at 4 M, pointed to the existence of di-, tri- and tetra-bromo complexes when the Br^-/Zn^{++} ratio was higher than 1.5. Frequencies characteristic for the three chemical species occur at 206, 183 and 171 cm^{-1}. In addition to the three polarized bands, zinc solutions showed a characteristic band at 382 cm^{-1} which is due to the symmetric stretching of zinc-hexaaquo complexes. The 1 : 4 complex was found to be tetrahedral, the 1 : 3 complex pyramidal with C_{3v} symmetry and the $ZnBr_2$ complex showed a bent structure with C_{2v} symmetry. No additional information could be deduced for the hydration of inner sphere complexes since the effective charge on Zn^{++} was not sufficient to produce an observable Raman intensity.

Contrary to zinc solutions recent X-ray diffraction studies of aqueous nickel bromide solutions with $Br^-/Ni^{++} = 2$ [3 – 4] and nickel chloride solutions with $Cl^-/Ni^{++} = 2.4$ [5], showed the presence of octahedral $Ni(H_2O)_6^{++}$ and $Ni[Br(H_2O)_5]^+$ as well as octahedral $Ni(H_2O)_6^{++}$, $Ni(H_2O)_5Cl^+$ and $Ni(H_2O)_4Cl_2$ complexes. The Cl^- in the 1 : 2 complexes were found in trans positions as in crystalline $NiCl_2 \cdot 6H_2O$.

The above results show some differences between the complex formation of the similar sized zinc and nickel ions. In order to reinvestigate the structure of bromide complexes of Zn^{++} we have measured the Raman spectra as well as the X-ray and electron scattering of an aqueous solution (1.64 molar in Zn^{++}) with a Br^-/Zn^{++} ratio of 3. The excess of

Reprint request to Dr. E. Kálmán, Central Research Institute for Chemistry, Hungarian Academy of Sciences, Pusztaszeri u. 59/67, H-1025 Budapest, Hungary.

0340-4811 / 83 / 0200-0225 $ 01.3 0/0. – Please order a reprint rather than making your own copy.

Table 1. Composition of the solutions investigated in mol/l. The values in parenthesis are mole fractions.

	Zn^{2+}	Br^-	ClO_4^-	NO_3^-	Li^+	Br^-/Zn^{2+}
A	1.64 (0.011)	5.06 (0.033)	–	–	3.09 (0.017)	3.08
B	3.0	–	6.0	–	–	–
C	6.7	–	–	13.4	–	–
D	6.7	2	–	13.4	2	0.3
E	3.3	3.3	–	6.6	3.3	1
F	1	10	–	2	10	10
G	3.5	7	–	–	–	2
H	10	20	–	–	–	2

bromide ions was achieved by the addition of LiBr. The composition of the solution (denoted by A) is given in Table 1.

2. The Raman spectra

In order to check the assignment of the bands in the spectra of the zinc bromide solutions by Macklin and Plane [2], we have measured Raman spectra of seven solutions including $Zn(ClO_4)_2$, $Zn(NO_3)_2$ and $ZnBr_2$ with and without excess of bromide ions. The compositions of these solutions (B–H) are given in Table 1. Raman spectra were excited with the 488 nm line of an ILA 120 argon ion laser. After passing the GDM 1000 double monochromator, the scattered light was recorded photoelectrically. $I_\parallel$ and $I_\perp$ spectra were obtained with fixed polarization of the laser beam by rotating an analyser between the sample and the entrance slit. $I_\parallel$ and $I_\perp$ spectra are proportional to $45\,\bar{\alpha}'^2 + 4\beta'^2$ and $3\beta'^2$ where all symbols have their usual meaning [6]. The precision of the frequencies is $\pm 1\ cm^{-1}$.

The isotropic spectra characteristic of zinc bromide complexes in the range $150-400\ cm^{-1}$ are shown in Figures 1 and 2. As has been expected [2], in the spectra of solutions of zinc perchlorate and zinc nitrate (B, C) only the band at $385\ cm^{-1}$ could be observed, which is due to the symmetric stretching vibration ν_{1g} of hexaaquo zinc complexes. Upon variation of the Br^-/Zn^{++} ratio in the range $0.3-10$ by addition of LiBr in $Zn(NO_3)_2$ solutions (D, E, F) bands appear at $172\ cm^{-1}$, $183\ cm^{-1}$ and $205\ cm^{-1}$ which can be assigned to the symmetric stretching vibration of the 1:4, 1:3 and 1:2 complexes. The band intensity increases with increasing Br^-/Zn^{++} ratio. A great excess of bromide ions (F) led only to one strong band at $172\ cm^{-1}$ with a shoulder at $185\ cm^{-1}$ indicating the predominance of tetrabromo complexes. No bands could be observed for hexaaquo and dibromo complexes. The spectra shown in Fig. 1 for zinc perchlorate and nitrate solutions support the assignments suggested by Macklin and Plane [2].

The spectra for zinc bromide solutions A, G and H (Table 1) are shown in Figure 2. In all spectra the symmetric stretching vibrations of hexaaquo, di-, tri- and tetrabromo complexes can be observed. The excess in bromide ions has led to increasing intensities of the tetrabromo band which is due to an increasing amount of $ZnBr_4^{--}$ complexes.

In order to convert the measured Raman intensities of the solution A to species concentration, it is necessary to know the integrated intensities of the bands I_ν and the molar intensities σ_ν of the components. The spectral contour of the three overlapping bands in the region of $130-250\ cm^{-1}$ was digital-

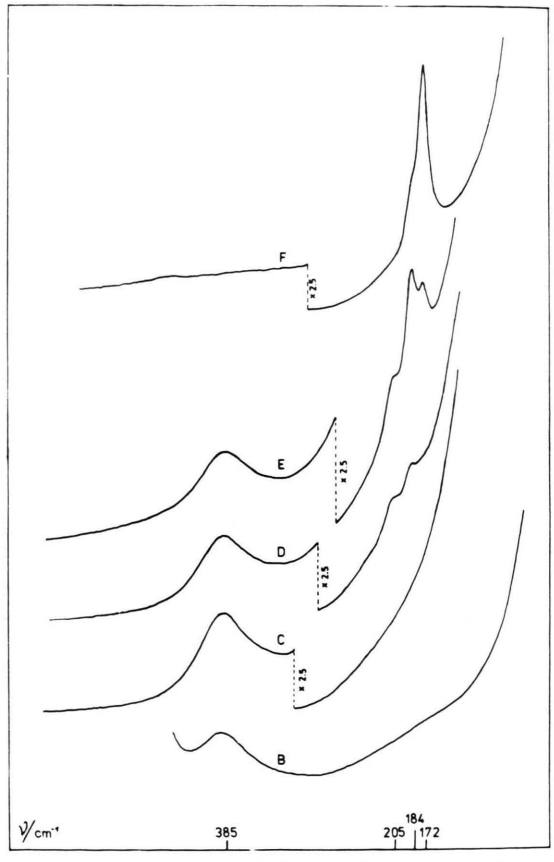

Fig. 1. Raman spectra of the solutions B–F (Table 1) in the region $150-400\ cm^{-1}$.

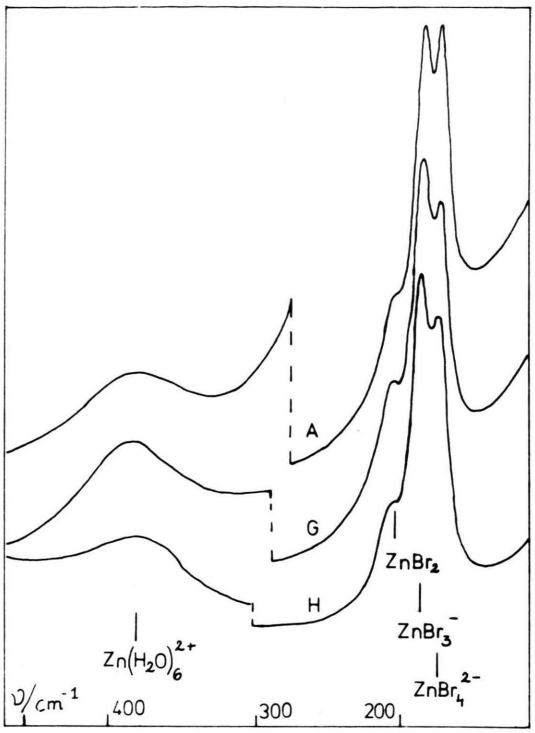

Fig. 2. Raman spectra of the solutions A, G and H Table 1) in the region 150 – 400 cm^{-1}.

ized and resolved into constituent components with Lorentz shape functions. The molar intensities of the three species were taken from the study of Macklin and Plane [2].

The resulted band parameters – band positions ν, half-widths $\beta\,\nu_{1/2}$, relative intensities I_ν, normalized intensities I_ν/σ_ν and the relative concentrations c_i – are given in Table 2. The ratio of the normalized intensities results in relative concentrations of the species as $[ZnBr_2] : [ZnBr_3^-] : [ZnBr_4^{2-}] = 1 : 1.75 : 1.14$. Because of the uncertainity limits for molar intensities [2], the relativ concentrations c_i can only be regarded as good estimations.

Table 2. Results of the Raman spectral investigations of solution A in the region 150 – 400 cm^{-1}. The symbols ν, $\Delta\nu_{1/2}$, I_ν, I_ν/σ_ν, c_ν are used to designate band positions, halfwidths, integrated relative intensities, normalized intensities and relativ concentrations, respectively.

	ν[cm^{-1}]	$\Delta\nu_{1/2}$[cm^{-1}]	I_ν	I_ν/σ_ν	C_ν
$ZnBr_2$	206	24	432	508	1
$ZnBr_3^-$	184	16	1600	888	1.75
$ZnBr_4^{2-}$	172	10	780	445	1.14

3. Electron and X-ray scattering

Structural parameters of the bromide complexes were determined by electron and X-ray scattering. The scattering cross section for 68 keV ($\lambda = 0.05$ Å) electrons was measured for solution A at 20 °C with a liquid electron-diffraction unit described in detail elsewhere [7]. Experimental data were collected over a range of the scattering variable $1\,Å^{-1} \leqq k \leqq 12.8\,Å^{-1}$, with $k = (4\pi/\lambda)\sin\vartheta$. In order to avoid predominance of scattering at small angles, a rotating sector was used. Diffraction patterns were recorded on Agfa-Gevaert Scientia photoplates. During the experiments the temperature and pressure in the chamber were controlled. Optical absorbancies measured with a microdensitometer were converted into intensities [8]. The measured intensities were corrected for extraneous scattering of the apparatus, for the sector shape and for the flat plates. The background scattering containing atomic self scattering, multiple scattering and inelastic-scattering was determined in an iterative process and refined together with structural parameters [8] and the normalization constant N.

The experimental structure function was determined by the following relation

$$H^E(k) = N\,\frac{(I^E(k) - I_B^E(k))}{[\sum x_\alpha f_\alpha^E(k)]^2}\,, \qquad (1)$$

where I^E, I_B^E, f_α^E are the corrected intensity, background intensity and electron scattering amplitudes of atoms or ions, respectively. α stands for Zn^{2+}, Br^-, Li^+, O and H.

The X-ray scattering intensity was measured on a $\theta - \theta$ diffractometer described previously [9]. The intensity of the diffracted radiation was measured at the discrete points 0.1° and 0.25° in the ranges $2° \leq \vartheta \leq 30°$ and $30° \leq \vartheta \leq 68°$ corresponding to a k range between 0.6 $Å^{-1}$ and 16.4 $Å^{-1}$. MoK_α radiation ($\lambda = 0.711$ Å) was used with a LiF single crystal monochromator placed between the sample and the scintillation counter. Experimental intensity data were corrected for background, absorption, polarization and Compton radiation. The corrected intensity was normalized by comparison with the total independent scattering using both integral and high angle methods. The coherent scattering amplitudes and anomalous dispersion corrections were taken from [10]. The experimental structure function

$H^x(k)$ was constructed according to the equation,

$$H^x(k) = \frac{I^x(k) - \sum_\alpha x_\alpha f_\alpha^{x^2}(k)}{[\sum_\alpha x_\alpha f_\alpha^x(k)]^2}, \quad (2)$$

where I^x is the corrected and normalized intensity, and f_α^x are the X-ray scattering amplitudes corrected for anomalous dispersion.

Radial distribution functions $D(r)$ representing the weighted distance spectrum of the solution for both electron and X-ray structure functions were calculated according to

$$D(r) = 4\pi r^2 \varrho_0 + \frac{2r}{\pi} \int_0^{k_{max}} k\, H(k) \sin(k\, r)\, dk, \quad (3)$$

where ϱ_0 is the average particle density of the solution.

In the calculated $D^E(r)$ and $D^x(r)$ peaks have appeared in the region below 1.8 Å due to intramolecular O–H distances of water molecules and long period spurious waves in structure functions. Since in this range no intermolecular interaction could appear, contributions were eliminated by repeated Fourier transformations. The structure functions are shown in Fig. 3 and the corresponding radial distribution functions for solution A in Figures 4 and 5.

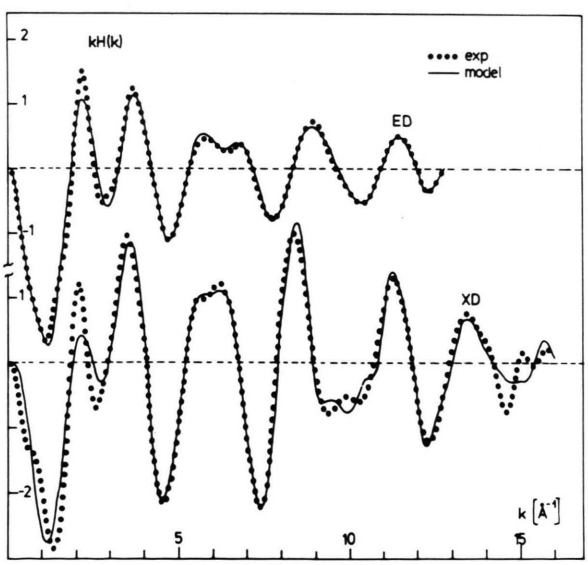

Fig. 3. Comparison of the structure functions for solution A from electron scattering and analytical fit (ED) and from X-ray experiment and analytical fit (XD).

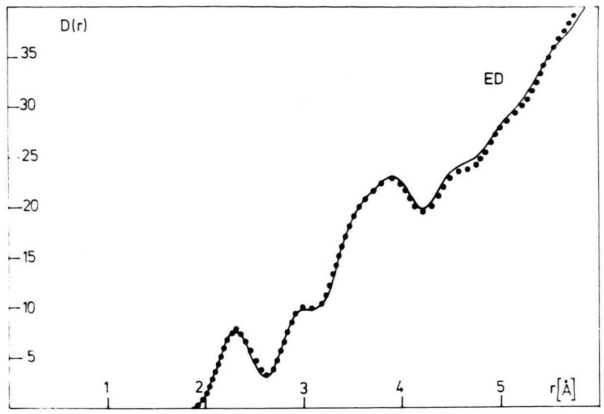

Fig. 4. Radial distribution function calculated from ED structure functions as given in Figure 3, $D^E(r)$.

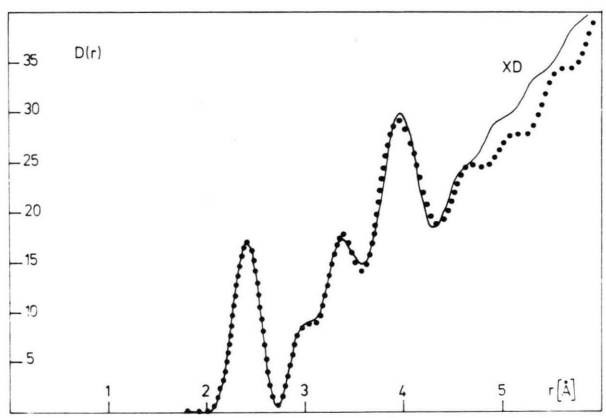

Fig. 5. Radial distribution function calculated from XD structure functions as given in Figure 3, $D^x(r)$.

Both radial distribution functions show peaks at 2.4 Å, 2.9 Å, and 3.9 Å. An additional peak exists in $D^x(r)$ at 3.4 Å which appears in $D^E(r)$ only as a shoulder. From the crystallographic radii of the ions the peaks at 2.4 Å, 2.9 Å, 3.4 Å, and 3.9 Å can be attributed to the Zn^{2+}–Br^-, H_2O–H_2O, Br^-–H_2O and Br^-–Br^- interactions, respectively. No resolved peak appears at 2.1 Å characteristic for Zn^{2+}–H_2O interactions in hexaaquo complexes found in aqueous $Zn(NO_3)_2$ [11] and $ZnSO_4$ [12, 13] solutions. In addition to the Raman spectra, these features of the radial distribution functions give also direct evidence for inner sphere complex formation. In order to evaluate the average structural parameters as mean distances and average coordination numbers of atoms, in a quantitative way the structure functions have to be analysed.

The experimental structure functions $H^i(k)$ $(i = \mathrm{E}, \mathrm{X})$ are determined by the $h_{\alpha\beta}(k)$ partial structure functions, which are in connection with the partial distance distributions of particles β around α,

$$H^i(k) = \sum_{\alpha} \sum_{\beta} \varrho_\beta \frac{x_\alpha f_\alpha^i(k) f_\beta^i(k)}{[\sum x_\alpha f_\alpha^i(k)]^2} h_{\alpha\beta}(k)\,, \qquad (4)$$

where ϱ_β is the number density of particle β.

In order to simplify Eq. (4), one can introduce two approximations. Firstly, it is enough to treat only Zn^{2+}–O, Br^-–O, O–O, Zn^{2+}–Br^- and Br^-–Br^- interactions because of the low coefficients for all other interactions. Secondly, we can restrict ourselves to nearest neighbour interactions and approximate the longer range correlations by continous distance spectra.

Using the latter approximation, the partial structure functions can be written in the following form

$$h^*_{\alpha\beta}(k) = \Delta_{\alpha\beta}(k) + \Omega_{\alpha\beta}(k) \qquad (5)$$

with

$$\Delta_{\alpha\beta}(k) = N_{\alpha\beta} \frac{\sin(k\, r_{\alpha\beta})}{k\, r_{\alpha\beta}} \exp\{-\, l^2_{\alpha\beta}\, k^2/2\}, \qquad (6)$$

$$\Omega_{\alpha\beta}(k) = \frac{4\pi}{k^3} (k\, R_{\alpha\beta} \cos(k\, R_{\alpha\beta}) - \sin(k\, R_{\alpha\beta})) \cdot \exp\{-\, L^2_{\alpha\beta}\, k^2/2\}, \qquad (7)$$

where $r_{\alpha\beta}$, $N_{\alpha\beta}$ and $l_{\alpha\beta}$ are the mean nearest neighbour distance between particles α and β, the mean number of particles β coordinating the particle α at distance $r_{\alpha\beta}$ and the root mean square deviations for mean distances $r_{\alpha\beta}$, respectively. The parameters $R_{\alpha\beta}$ and $L_{\alpha\beta}$ are characteristic for the boundary of the structured environment. Least squares refinements of the structural parameters were performed by minimizing the following expression both for X-ray and electron scattering data,

$$\sigma^2 = \sum_i k_i^2 [H(k_i) - H^*(k_i)]^2\,. \qquad (8)$$

The comparison of the experimental structure functions with the final calculated structure functions is given in Figure 3. The resulting structural parameters calculated from X-ray and electron structure functions are given in Table 3.

Table 3. Mean distances $r_{\alpha\beta}$[Å], r.m.s. variations $l_{\alpha\beta}$[Å] and coordination numbers $N_{\alpha\beta}$ for nearest neighbour interactions obtained from the electron (E) and the X-ray (X) structure function.

		$r_{\alpha\beta}$	$l_{\alpha\beta}$	$N_{\alpha\beta}$	$R_{\alpha\beta}$	$L_{\alpha\beta}$
E	Zn^{2+}–O	2.23	0.083	2.40	2.63	0.05
	Zn^{2+}–Br^-	2.40	0.126	2.22	3.48	0.01
	O–O	2.93	0.102	1.12	2.88	0.29
	Br^-–O	3.49	0.195	4.36	3.26	0.19
	Br^-–Br^-	3.91	0.116	1.36	5.27	0.15
X	Zn^{2+}–O	2.21	0.093	2.42	3.06	0.09
	Zn^{2+}–Br	2.42	0.116	2.26	3.69	0.02
	O–O	2.90	0.082	1.09	2.83	0.21
	Br^-–O	3.45	0.25	4.20	3.36	0.13
	Br^-–Br^-	3.95	0.132	1.28	4.83	0.17

4. Discussion of the results

A quite good agreement exists between the experimental and fitted structure functions except in the range of the first maximum (Figure 3). The discrepancies at a k-value of about $2\,\text{Å}^{-1}$ can be attributed to the limitations of the nearest neighbour approximation for the partial structure functions. The experimental radial distribution functions in the range of the nearest neighbour interactions (2 Å – 4 Å) are well reproduced by fitted ones (Figs. 4, 5). The structural parameters (Table 3) is obtained from the two independent diffraction experiments are in good agreement, which supports their reliability. The bond distance of Zn^{2+}–Br^- indicates that the bromo complex belongs to the inner type of coordination. Its value of 2.41 Å is significantly smaller than the expected one from ionic radii, 2.65 Å. A similar phenomenon was observed for Ni^{2+}–Br^- interactions in the aqueous $NiBr_2$ solutions [3]. The bond distance of 2.22 Å for Zn^{2+}–H_2O contact is greater than that for the hexaaquo complexe in $Zn(NO_3)_2$ [11] and $ZnSO_4$ [12] solutions. The r.m.s. variations of the mean distances, $l_{\alpha\beta}$, are in general low, except for Br^-–O interactions. The low values of $l_{\alpha\beta}$ indicate strong interactions between the particles, which are characteristic for complex formation [14–17]. The value of 2.2 for the average number of zinc-bromide contact, results in a concentration of about 1.4 mol/l for free hydrated bromide ions. Mean coordination numbers given in Table 3 are not far from those characteristic for $ZnBr_2(H_2O)_2$ complexes ($N_{Zn-O} = 2$, $N_{Zn-Br} = 2$, $N_{O-O} = 1$, $N_{Br-Br} = 1$). However, the significance of deviations between these parameters is supported by the fact that similar values resulted from both type of diffraction experiments.

Table 4. Estimated concentrations of complex species in solution A C_{diff} and C_{Raman} are calculated from diffraction and Raman data, respectively.

	$[Zn(H_2O)_6]^{2+}$	$[ZnBr_2(H_2O)_2]$	$[ZnBr_3(H_2O)]^-$	$[ZnBr_4]^{2-}$
C_{diff}	0.25	0.25	0.35	0.15
C_{Raman}	0.28	0.19	0.33	0.21

The independent refinement of the Zn^{2+}–Br^- and the Br^-–Br^- interactions leads to a tetrahedral Br–Zn–Br angle. This result (together with the low values found for Zn^{2+}–O and O–O contacts) strongly indicates formation of a tetrahedral inner sphere complex.

If we assume – based on Raman spectra – that the dominant species in the solution are the hexaaquo and tetrahedral $ZnBr_2(H_2O)_2$, $ZnBr_3H_2O^-$ and $ZnBr_4^{2-}$ complexes, their concentrations can be estimated easily. The resulting coordination numbers are in good agreement with those obtained from diffraction experiments. Similarly, assuming from the diffraction data, that the average number of zinc-bromide contacts is 2.2, the relative concentrations c_0 calculated from Raman spectra for 1 : 2, 1 : 3, 1 : 4 complexes can be converted to absolute values. The agreement between concentrations estimated in both ways is relatively good (Table 4).

The mean value of nearest Br–O distances, 3.47 Å, is slightly greater than that got for aqueous $NiBr_2$ solutions [3] and deviates significantly from that in HBr solutions [18]. The $r_{Zn^{2+}-O}$ and r_{Br^--O} distances are averaged values of distances in hydrated ions and bromide complexes. Thus the higher values found can possibly be explained by increased values of the distances in the complexes. The mean value of 4.3 Å for bromide-oxygen contacts together with the estimated concentration of about 1.4 mol/l for hydrated bromide ions gives a value of 7.3 for the coordination number of free bromide ions.

Acknowledgement

The authors are grateful to Mr. L. Haklik for technical assistance and Mr. P. Kovács for computational assistance in the electron diffraction experiment and are indebted to Mrs. E. Tarlós for preparation of the manuscript.

[1] D. L. Wertz, R. M. Lawrence, and R. F. Kruh, J. Chem. Phys. **43,** 2163 (1965).
[2] J. W. Macklin and R. A. Plane, Inorg. Chem. **9,** 821 (1970).
[3] H. Wakita, M. Ichihashi, T. Mibuchi, and I. Masuda, Bull. Chem. Soc. Japan **55,** 817 (1982).
[4] R. Caminiti and P. Cucca, Chem. Phys. Lett. **89,** 110 (1982).
[5] M. Magini, G. Paschina, and G. Piccaluga, J. Chem. Phys. **76,** 1116 (1982).
[6] J. R. Scherer, M. K. Go, and S. Kint, J. Phys. Chem. **78,** 1304 (1974).
[7] E. Kálmán, S. Lengyel, L. Haklik, and A. Eke, J. Appl. Cryst. **7,** 442 (1974).
[8] E. Kálmán, G. Pálinkás, and P. Kovács, Mol. Phys. **34,** 505 (1977).
[9] G. Johansson, Acta Chem. Scand. **20,** 553 (1966).
[10] International Tables for X-ray Crystallography, Vols 3 and 4. Kynoch Press, Birmingham 1968 and 1974.
[11] W. Bol, G. Gerrits, and C. van Panthaleon van Eck, J. Appl. Cryst. **3,** 486 (1970).
[12] T. Radnai, G. Pálinkás, and R. Caminiti, Z. Naturforsch. **37a,** Heft 11 (1982).
[13] H. Ohtaki, T. Yamaguchi, and M. Maeda, Bull. Chem. Soc. Japan **49,** 701 (1976).
[14] M. Magini, J. Chem. Phys. **74,** 2523 (1981).
[15] M. Maeda, H. Ohtaki, and G. Johansson, Bull. Chem. Soc. Japan **47,** 2229 (1974).
[16] M. Magini and T. Radnai, J. Chem. Phys. **71,** 4255 (1979).
[17] S. Lengyel, Annales Univ. Sci. Budapest **1,** 96 (1959).
[18] N. Ohtomo, K. Arakawa, M. Takeuchi, T. Yamaguchi, and H. Ohtaki, Bull. Chem. Soc. Japan **54,** 1314 (1981).